JOURNAL OF SOLID STATE CHEMISTRY 97, 466–475 (1992)

The Effect of Heat Treatments on Cobalt Configuration and Physical Properties of $YBa_2(Cu_{1-x}Co_x)_3O_y$

S. KATSUYAMA

Department of Materials Science and Engineering, Faculty of Engineering, Osaka University, Suita Osaka 565, Japan

S. NASU

Department of Materials Physics, Faculty of Engineering Science, Osaka University, Toyonaka Osaka 560, Japan

Y. UEDA

Institute for Solid State Physics, University of Tokyo, Tokyo 106, Japan

AND K. KOSUGE

Department of Chemistry, Faculty of Science, Kyoto University, Kyoto 606, Japan

Received August 8, 1991; in revised form October 22, 1991

$YBa_2(Cu_{1-x}Co_x)_3O_y$ ($0 \leqq x \leqq \frac{1}{3}$) was prepared by two kinds of heat treatments: (a) slow cooling from 850°C in flowing O_2 gas and (b) reducing at 800°C in flowing N_2 gas followed by reoxidation in flowing O_2 gas below 400°C. The crystal structure, superconducting properties, and Co configuration of the materials were examined by X-ray powder diffraction, electrical resistivity, and ^{57}Co emission Mössbauer measurements. The orthorhombic phase was stabilized in the wide composition range ($0 \leqq x \leqq 0.12$) by the heat treatment (b) as well as in the Fe-substituted system. This extension of the orthorhombic phase region is due to the clustering of Co atoms in the Cu1–O planes, which is developed by the heat treatment under a lower oxygen fugacity atmosphere at high temperature. © 1992 Academic Press, Inc.

Introduction

It is well known that the substitution for Cu in $YBa_2Cu_3O_y$ by other metals such as Fe, Co, Ni, Zn, etc., has effects upon its crystal structure and superconducting properties. Such substitution reduces the superconducting transition temperature, *Tc*, and the substitution by Fe and Co induces an orthorhombic-to-tetragonal structural phase transition (*1–5*). In the previous papers, we reported that such substitution effect is strongly affected by the thermal treatment (*6–8*). For example, $YBa_2(Cu_{1-x}Fe_x)_3O_y$ prepared by slow cooling from 850°C in flowing O_2 gas undergoes the phase transition from the orthorhombic to the tetragonal structure at about $x =$

0022-4596/92 $3.00

0.03 and Tc decreases with increase of x, while the heat treatment of reducing in flowing N_2 gas at 800°C followed by reoxidation in flowing O_2 gas below 400°C stabilizes the orthorhombic phase in the wide composition range ($0 \leqq x \leqq 0.15$) and Tc^{onset} of this orthorhombic phase is about 85 K independent of x. From the systematic studies of ^{57}Fe Mössbauer spectroscopy and ac susceptibility measurements, we ascribed these phenomena to the clustering of Fe atoms in the Cu(1)–O planes (between two BaO layers), which is developed by the heat treatment under an atmosphere of lower oxygen fugacity at high temperature (*6–8*).

Thus, the crystal structure and superconducting properties of $YBa_2(Cu_{1-x}Fe_x)_3O_y$ are closely related to the microscopic structure of the substituent in the crystal. It is interesting to examine the effect of thermal treatment on the crystal structure and superconducting properties of $YBa_2(Cu_{1-x}Co_x)_3O_y$ and compare the results with those of the Fe-substituted system. In this paper, we report the results of the X-ray diffraction, electrical resistivity, and ^{57}Co emission Mössbauer measurements on $YBa_2(Cu_{1-x}Co_x)_3O_y$ and discuss the results from the standpoint of the microscopic configuration of Co atoms in the crystal.

Experimental

The starting compound of $YBa_2(Cu_{1-x}Co_x)_3O_y$ ($0 \leqq x \leqq \frac{1}{3}$) was prepared by the solid state reaction of 4N-Y_2O_3, $BaCO_3$, CuO, and CoO at 900°C in air. The prepared compounds were divided into two parts and were offered to the heat treatments as shown in Fig. 1. Here, [O] is the ordinary oxidizing treatment and [NO] is the reduction by high purity nitrogen gas at high temperature ([N]) followed by reoxidation at low temperature. The phase identification of the samples was made by X-ray diffraction at room temperature.

The superconducting properties of the samples were examined by electrical resistivity measurements by use of the standard four-probe method.

For the ^{57}Co emission Mössbauer measurement, two pellets of the starting compound with diameter of about 10 mm and thickness of about 1.5 mm were sintered at 900°C for 24 hr in air. About 15 μl of 0.1 N hydrochloric acid solution of $^{57}CoCl_2$ (including about 37 MBq ^{57}Co) was dropped on each sintered pellet. The dried pellets were heated at 900°C for 3 hr in flowing O_2 gas to diffuse ^{57}Co into the materials and slowly cooled to the room temperature in 14 hr under the same atmosphere. Then one of the pellets was treated by [NO]. Mössbauer measurement was done on the pellet-formed samples at room temperature. Emission spectra were recorded using a single line absorption of ^{57}Fe in Pd matrix. The sign of the velocities was reversed to correspond to an absorption experiment. The isomer shift is given with respect to bcc Fe.

Results

1. Phase Identification

Figures 2(a), (b), and (c) show lattice parameters vs x in $YBa_2(Cu_{1-x}Co_x)_3O_y$ for the samples $[O]_s$, $[N]_s$, and $[NO]_s$, respectively, where $[O]_s$, $[N]_s$, and $[NO]_s$ denote the samples prepared by the heat treatments of [O], [N], and [NO], respectively. The phase transition from the orthorhombic to tetragonal structure takes place at about $x = 0.04$ in $[O]_s$, which agrees with the results of many other works (*1–5*). The crystal structure of the samples obtained by [N] is tetragonal in the whole range of x investigated. This tetragonal phase is an oxygen deficient one. On the other hand, the crystal structure of $[NO]_s$ is orthorhom-

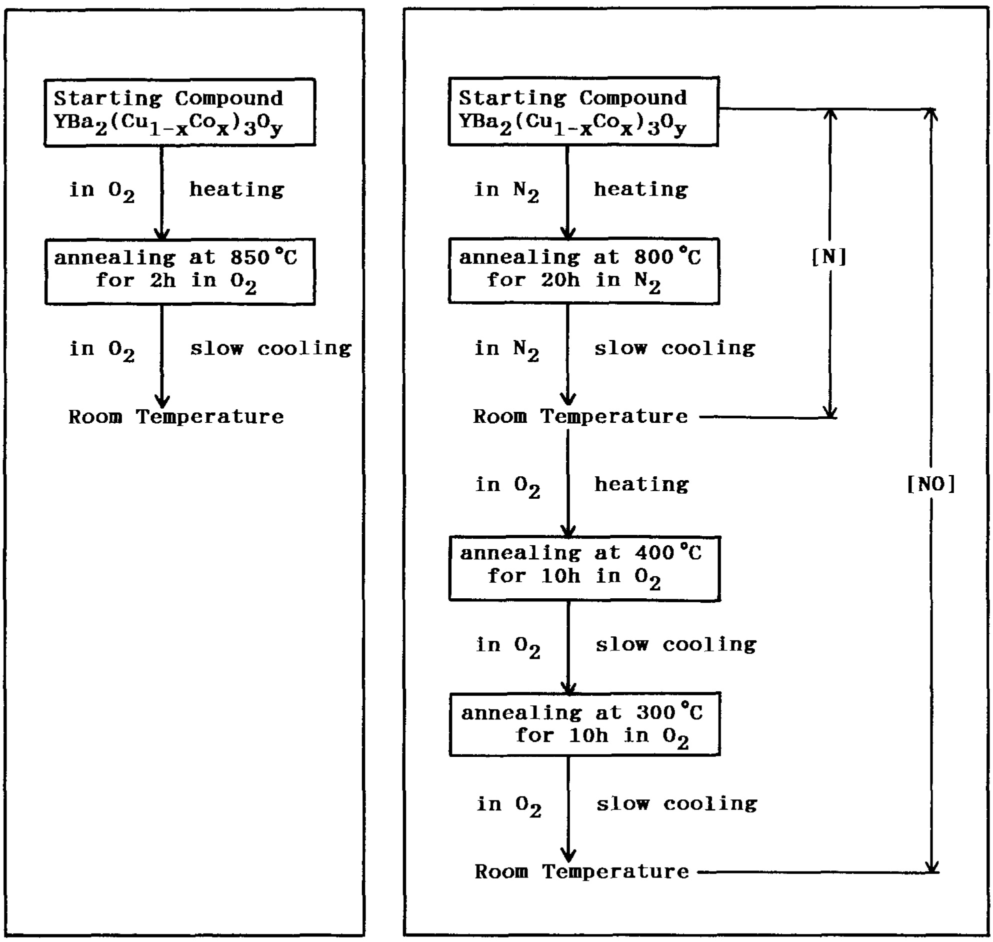

Heat Treatment of [O]

Heat Treatments of [N] and [NO]

FIG. 1. Flow chart of the heat treatments of [O], [N], and [NO].

bic up to $x = 0.12$. In the whole range of x investigated ($0 \leqq x \leqq \frac{1}{3}$), no second phase was recognized.

2. *Superconducting Properties*

The x-dependence of Tc, together with the width ΔTc, is shown in Figs. 3(a) and (b) for $[O]_s$ and $[NO]_s$. Tc for both $[O]_s$ and $[NO]_s$ decreases monotonously with increase of x. Comparing Tc between $[O]_s$ and $[NO]_s$ at fixed composition of x, Tc of $[O]_s$ is higher than that of $[NO]_s$.

3. *^{57}Co Emission Mössbauer Effect*

Figures 4(a), (b), and (c) show ^{57}Co emission Mössbauer spectra of $[O]_s$, $[NO]_s$, and $[N]_s$, respectively.

The spectra for $[O]_s$ and $[NO]_s$ can be analyzed to consist of four sets of quadrupole doublets (D-1, D-2, D-3, and D-4). The Mössbauer parameters of these subspectra are almost the same as those for $[O]_s$ and $[NO]_s$ of the Fe-doped $YBa_2Cu_3O_y$ (see Table I). The spectrum for $[N]_s$ is also analyzed into four components, i.e., three sets of

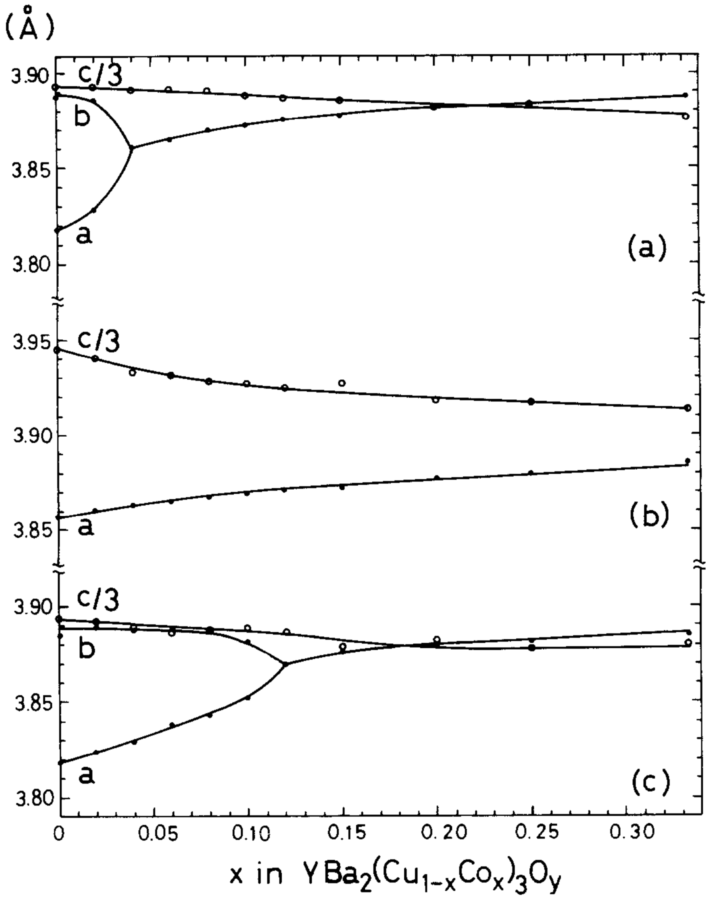

FIG. 2. Lattice parameters vs x curves for $YBa_2(Cu_{1-x}Co_x)_3O_y$: (a) $[O]_s$, (b) $[N]_s$, and (c) $[NO]_s$.

quadrupole doublets (D-5, D-6, and D-7) and one magnetically splitted sextet (S-1). The Mössbauer parameters and relative intensities of each component are summarized in Table I, together with those of $YBa_2(Cu_{0.96}Fe_{0.04})_3O_y$ in the previous study. There are some differences about the values of Mössbauer parameters for $[N]_s$ between the Co- and Fe-doped $YBa_2Cu_3O_y$. The asymmetry in peak intensities indicates that there is some degree of orientation in microcrystallites, since the measurement was done on pellet-formed samples. In the spectra for $[O]_s$ the D-1 component is a main one, while in the spectra for $[NO]_s$ the D-2 and D-3 components grow.

Discussion

We previously examined the effect of the thermal treatments on the crystal structure and superconducting properties of $YBa_2(Cu_{1-x}Co_x)_3O_y$ (*6–8*). As a result, it became clear that its crystal structure and superconducting properties are closely related to the microscopic arrangement of the substituent in the crystal, for example, the distribution of the substituent between the Cu1 and Cu2 sites, intra-plane location of the substituent, and the local oxygen ordering.

Many studies have been done to solve the problem of which site (Cu1 or Cu2) in $YBa_2(Cu_{1-x}Co_x)_3O_y$ is occupied by the sub-

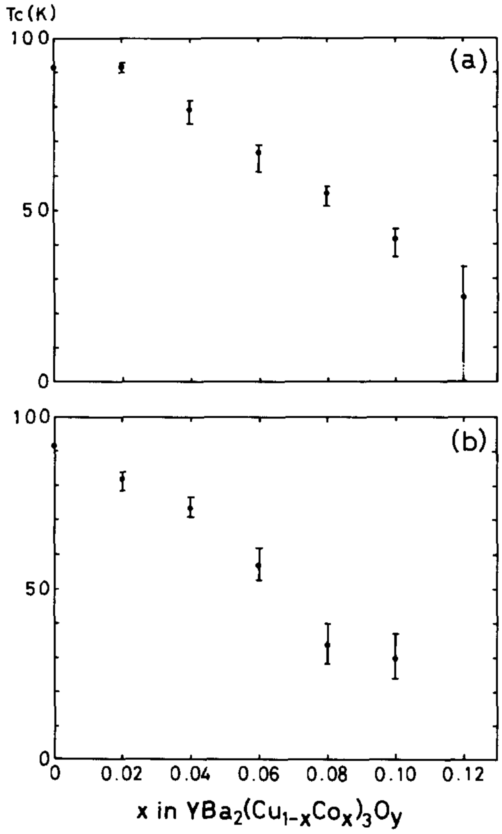

FIG. 3. Cobalt concentration dependence of the superconducting transition temperature Tc for (a) $[O]_s$ and (b) $[NO]_s$. The closed circles show the midpoint of the transition, and the top and bottom of the bars correspond to the temperature with 90 and 10% values of the normal state resistivity.

stituted Co atoms. From the orthorhombic-to-tetragonal phase transition caused by the substitution of Co atoms, it was expected that Co atoms are mainly substituted for Cu in the Cu1 sites, since this transition is considered to be induced by oxygen disordering in the Cu1–O plane, which is introduced by extra oxygen atoms around the substituted atoms in the Cu1 site (*5*). In fact, the neutron diffraction and EXAFS measurements have revealed that Co atoms are mainly located in the Cu1 site (*9–12*). Here, we discuss the distribution of Co atoms on the basis of the analysis of the ^{57}Co emission Mössbauer spectra for $YBa_2(Cu_{1-x}Co_x)_3O_y$.

In the previous study about the ^{57}Fe absorption Mössbauer measurement of $YBa_2(Cu_{1-x}Fe_x)_3O_y$, we ascribed the magnetically splitted sextet in the reduced sample $[N]_s$ to the Fe located in the Cu2 site, since the Cu atom in the Cu2 site of the oxygen-deficient $YBa_2Cu_3O_6$ shows an antiferromagnetic long range order with T_N of about 400 K, which has been established from the neutron diffraction and NMR studies (*13, 14*). Sedykh *et al.* observed that this magnetic sextet was converted to a paramagnetic doublet which was identical to the D-3 component in the oxidized sample above 420 K (*15*). It is reasonable that the magnetically splitted sextet in the spectrum for $[N]_s$ and the D-3 component in the spectra for $[O]_s$ and $[NO]_s$ in the Co-substituted system are also ascribed to the Co atoms located in the Cu2 site. The other components (D-1, D-2, D-4, D-5, D-6, and D-7) are attributed to the Co atoms with various oxygen coordinations in the Cu1 site.

From the above analysis, it is apparent that about 97% of the total Co atoms in the crystal of $[O]_s$ are located in the Cu1 site, which is consistent with the result of the neutron diffraction and EXAFS measurements that Co atoms in $YBa_2(Cu_{1-x}Co_x)_3O_y$ are mainly located in the Cu1 site (*9–12*). The proportion of the Co atom located in the Cu2 site grows in $[N]_s$ and $[NO]_s$. As shown in Table I, this behavior was also observed in the Fe-substituted system. Comparing with the Fe-substituted system, it can be said that both Co and Fe tend to occupy the Cu1 site but the tendency is stronger in Co.

Next we discuss the oxygen coordination around the Co atoms in the Cu1 site. Nasu and co-workers prepared a powder specimen of $YBa_2(Cu_{1-x}Fe_x)_3O_y$ fixed in glue under an external magnetic field of 1.8 T to have a strong texture along the *c*-axis and measured the dependence of the asymmetry

TABLE I

^{57}Co Emission and ^{57}Fe Absorption Mössbauer Parameters Obtained from $YBa_2(Cu_{0.96}Co_{0.04})_3O_y$, $Yba_2Cu_3O_y$, and $Yba_2(Cu_{0.96}Fe_{0.04})_3O_y$ at Room Temperature

	^{57}Co Emission Mössbauer												^{57}Fe Absorption Mössbauer								
	$YBa_2(Cu_{0.96}Co_{0.04})_3O_y$									$YBa_2Cu_3O_y$			$YBa_2(Cu_{0.96}Fe_{0.04})_3O_y$								
	$[O]_s$			$[NO]_s$			$[N]_s$			$[N]_s$			$[O]_s$			$[NO]_s$			$[N]_s$		
	δ	Δ	A	δ	Δ	A	δ	Δ	A	δ	Δ	A	δ	Δ	A	δ	Δ	A	δ	Δ	A
D-1	−0.08	1.94	68	−0.07	1.87	31							0.04	1.87	33	0.04	1.97	4			
D-2	−0.06	1.10	9	−0.06	0.96	27							−0.03	1.04	44	0.00	1.00	63			
D-3	0.24	0.63	3	0.20	0.57	40							0.36	0.63	13	0.28	0.56	33			
D-4	−0.24	1.49	20	−0.20	1.59	2							−0.17	1.56	10	—	—	—			
D-5							−0.05	2.02	49	0.05	1.94	7									
D-6							−0.26	0.61	6	—	—	—									
D-7							0.12	0.87	8	0.27	0.96	13									
S-1							0.32	−0.30	37	0.15	−0.29	80									
D-8																			0.08	2.14	12
D-9																			0.07	1.13	33
D-10																			0.31	1.27	21
S-2																			0.45	−0.27	34

Note. δ is the isomer shift relative to bcc Fe at room temperature (mm/sec); Δ is the quadrupole splitting (mm/sec); and A is the relative intensity (%).

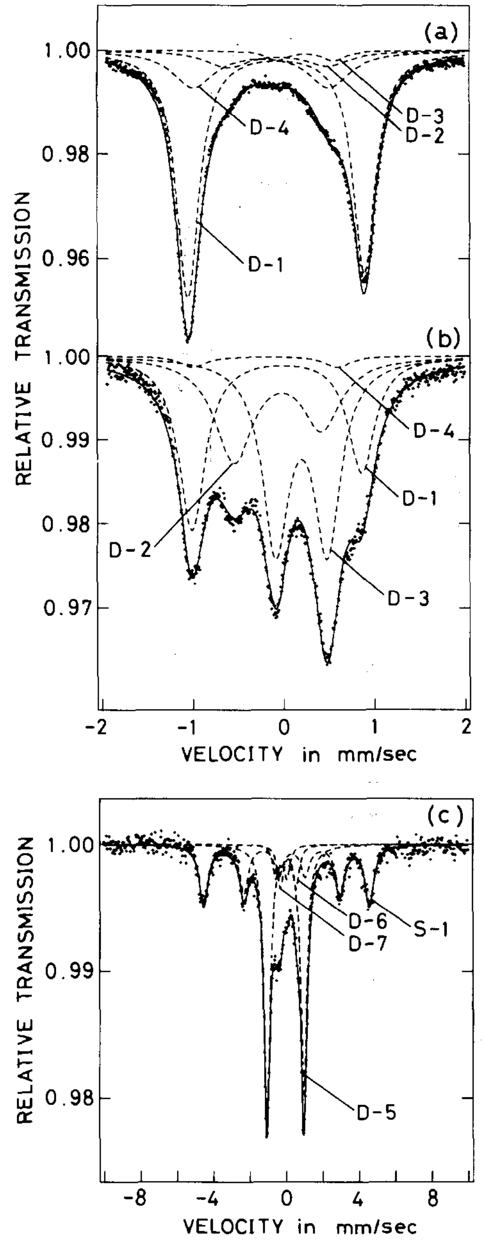

FIG. 4. ^{57}Co emission Mössbauer spectra of ^{57}Co-doped $YBa_2(Cu_{0.96}Co_{0.04})_3O_y$ at room temperature: (a) $[O]_s$, (b) $[NO]_s$, and (c) $[N]_s$. The velocity scale is relative to bcc Fe at room temperature and converted its sign for the absorption experiment.

of the ^{57}Fe absorption Mössbauer spectrum on the angle between the gamma-ray direction and c-axis *(16–18)*. From the experiment, they determined the direction of the magnetic moment and the sign and principle axis of the electric field gradient tensor of each component and proposed that the D-1 component is attributed to the Fe with tetrahedral four oxygen coordination, while the D-2 component to the Fe with octahedral six oxygen coordination.

According to the same site assignment, about 68% of the Co atoms in the Cu1 site of $[O]_s$ have tetrahedral coordination and about 9% have octahedral coordination. This result is in contrast to the result in the Fe-substituted system, where about 37% of the Fe atoms in the Cu1 site have tetrahedral coordination and 49% have octahedral coordination. This shows that Co atoms in the Cu1 site have a stronger tendency to favor tetrahedral coordination than do Fe atoms. In fact, the oxygen content y in $[O]_s$ estimated from the neutron diffraction is smaller in $YBa_2(Cu_{0.94}Co_{0.06})_3O_y$ ($y = 6.93$) than in $YBa_2(Cu_{0.94}Fe_{0.06})_3O_y$ ($y = 7.01$) *(19)*. In $[NO]_s$ the proportion of the Co atoms with octahedral coordination grows larger, but, is not so large as that of the Fe atoms with octahedral coordination in $[NO]_s$ of $YBa_2(Cu_{1-x}Fe_x)_3O_y$. The tendency that a Co atom is apt to have tetrahedral coordination is also observed in $[NO]_s$.

Thus, the distribution of the substituents between two Cu sites (Cu1 and Cu2) and the oxygen coordination around the substituents in the Cu1 site are affected by the heat treatments. Such configuration of the substituents is closely related to the crystal structure and superconducting properties of the materials. In previous papers we reported that the orthorhombic phase in $YBa_2(Cu_{1-x}Fe_x)_3O_y$ was stabilized by [NO] over the wide composition range of x *(6–8)*. We proposed that the clustering of Fe atoms in the Cu1–O planes is prevalent for the large extension of the orthorhombic region in $[NO]_s$. The transition from the orthorhombic to the tetragonal phase accompanied with the substitution by impurity is generally considered to be caused by extra oxygens strongly bound to the substituted atoms in the Cu1 sites which favor five or six oxygen coordination (*5*). These extra oxygens occupy ($\frac{1}{2}$ 0 0) site and induce the local disordering of oxygen in the Cu1–O planes. Since the substituted atoms in $[O]_s$ are randomly distributed in the Cu1–O planes, the Cu1–O planes are divided into a number of orthorhombic domains with smaller size; with increase of the concentration of the substituent in the Cu1–O plane the orthorhombic domains become small in size, and above a critical concentration an average structure is identified to be tetragonal but not orthorhombic by X-ray diffraction. Under a reducing atmosphere such as in flowing N_2 gas at high temperature the oxygens in the Cu1–O planes are removed. In this situation some of the Fe atoms in the Cu1 site move to the Cu2 site where the Fe atoms can have five oxygen coordination and the remaining Fe atoms in the Cu1–O plane may be clustered together, since the clustered substituents are able to keep five or six oxygen coordination by sharing oxygen atoms even under much lower total oxygen content than in the case of the isolated substituent. The reoxidation at low temperature, where the clustered state is frozen, enlarges the size of the orthorhombic domains, and the materials are again characterized to be as orthorhombic phase.

In the Co-substituted system the orthorhombic region was extended by [NO] up to $x = 0.12$. The intensity of both D-3 and D-2 components in the Mössbauer spectrum for $[NO]_s$ is stronger than that for $[O]_s$. The increase of the intensity of D-3 component in $[NO]_s$ is explained to be due to the movement of the Co atoms from the Cu1 to Cu2 site, and that of the D-2 component, which is attributed to the Co atoms with octahedral coordination, can be understood as the result of the clustering of the Co atoms in the Cu1–O planes during the reduction at high temperature.

Some workers also have investigated the effect of the thermal treatments on the physical properties of Fe-doped $YBa_2Cu_3O_y$ (*23, 24*). Smith *et al.* proposed that the Fe–O cluster formation in the Cu1–O plane is produced by annealing in flowing N_2 gas at 770°C for 48 hr, though they thought that the Fe atoms with fivefold oxygen coordination share the oxygen atoms in the Fe clusters (*24*).

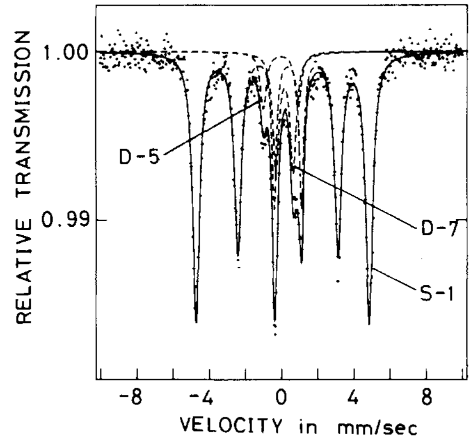

FIG. 5. ^{57}Co emission Mössbauer spectrum of ^{57}Co-doped $Yba_2Cu_3O_6$ semiconductor prepared by the heat treatment [N].

In discussing the relation between the distribution and the oxygen coordination of the Co atoms, the result of the source experiment using a 37 MBq ^{57}Co-doped $YBa_2Cu_3O_y$ is very interesting (*16*). Figure 5 shows the ^{57}Co emission Mössbauer spectrum for $[N]_s$ of $YBa_2Cu_3O_6$. The spectrum consists of three components, i.e., two sets of quadrupole doublets (D-5 and D-7) and one magnetically splitted sextet (S-1). It is noted that the intensity ratio of the magnetically splitted sextet in the spectrum for $YBa_2Cu_3O_y$ is much higher than that for $YBa_2(Cu_{0.96}Co_{0.04})_3O_y$. The latter is about 37%, while the former is about 80%. A similar result was reported by Nath *et al.* (*20, 21*). They prepared the ^{57}Co-doped $YBa_2Cu_3O_y$ by reducing in flowing N_2 gas at 700°C for 2 hr and observed the magnetically splitted sextet component whose relative intensity in the spectrum is about 65%. They realized that this magnetically splitted sextet is assigned to the Co atoms in the Cu1 site with just two oxygen atoms as neighbors along the *c* axis. This assignment is different from ours. Considering that the Co atoms prefer high oxygen coordination, we can understand this phenomenon as follows; it is difficult for the Co atoms in the Cu1 site in a 37 MBq ^{57}Co-doped $YBa_2Cu_3O_y$ to make a cluster because of the extremely low concentration of Co atoms, and most of the Co atoms in the Cu1 sites move to the Cu2 sites where the Co atoms can have five oxygen coordination.

Thus, the results of X-ray diffraction and Mössbauer measurements definitely indicate that the Co atoms in the Cu1–O plane in $[NO]_s$ make clusters. On the other hand, the Tc determined by the electrical resistivity measurement decreases monotonously with increase of the Co content x in $[O]_s$ as well as $[NO]_s$, and Tc of $[NO]_s$ is lower than that of $[O]_s$ at fixed composition of x. This result seems to be in contrast to the result of the Fe-substituted system. In the Fe-substituted system, Tc^{onset} of $[NO]_s$ is about 85 K independent of x (*6–8*). Our recent study by means of ac susceptibility shows that the Meissner effect of $[NO]_s$ of $YBa_2(Cu_{0.94}Co_{0.06})_3O_y$ begins at about 70 K, which is much higher than the Tc^{onset} determined by the electrical resistivity measurement (*22*). This suggests the existence of the superconducting region with higher Tc in $[NO]_s$, though the volume fraction of this region is very small. These behaviors can be referred to the clustering of the Co atoms in the Cu1–O planes in $[NO]_s$ as well as in the case of the Fe-substituted system.

There seem to be some differences in the configuration of the substituents between the Co- and Fe-substituted systems. As mentioned above, Fe atoms in the Cu1 site have a stronger tendency to have high oxygen coordination than do Co atoms. The proportion of the substituents with octahedral coordination in the Cu1–O plane of $[NO]_s$ is much larger in the Fe-substituted system than in the Co-substituted system; about 94% of the Fe atoms located in the Cu1 site have octahedral coordination, while about 45% of the Co atoms do. This result may indicate that there is a difference in the morphology of the clustering between the Co- and Fe-substituted systems; also, a difference of the volume fraction of the superconducting region between the Co- and Fe-substituted systems, especially in $[NO]_s$, may be referred to the difference in the morphology of the clustering in the Cu1–O plane between these two systems. There is a possibility that the difference in the configuration of the substituents in the Cu2–O plane affects the superconducting properties of the samples.

In conclusion, the microscopic study of the substituents is an indispensable key to solve the above problems, and so we are now studying by NMR and electron microscopy.

Acknowledgment

We thank Mr. M. Komazawa for the measurements of X-ray diffraction and electrical resistivity.

References

1. Y. Maeno, T. Tomita, M. Kyogoku, S. Awaji, Y. Aoki, K. Hoshino, A. Minami, and T. Fujita, *Nature* **328,** 512 (1987).
2. G. Xiao, F. H. Streitz, A. Gavrin, Y. W. Du, and C. L. Chien, *Phys. Rev. B: Condens. Matter* **35,** 8782 (1987).
3. D. Shindo, K. Hiraga, M. Hirabayashi, A. Tokiwa, M. Kikuchi, Y. Shono, O. Nakatsu, N. Kobayashi, Y. Muto, and E. Aoyagi, *Jpn. J. Appl. Phys.* **26,** L1667 (1987).
4. J. M. Tarascon, P. Barboux, P. F. Miceli, L. H. Greene, and G. W. Hull, *Phys. Rev. B: Condens. Matter* **37,** 7458 (1988).
5. Y. Oda, H. Fujita, H. Toyoda, T. Kaneko, T. Kohara, I. Nakada, and K. Asayama, *Jpn. J. Appl. Phys.* **26,** L1660 (1987).
6. S. Katsuyama, Y. Ueda, and K. Kosuge, *Mater. Res. Bull.* **24,** 603 (1989).

7. S. Katsuyama, Y. Ueda, and K. Kosuge, *Physica C* **165,** 404 (1990).

8. H. Mazaki, S. Katsuyama, H. Yasuoka, Y. Ueda, and K. Kosuge, *Jpn. J. Appl. Phys.* **28,** L1909 (1989).

9. T. Kajitani, K. Kusaba, M. Kikuchi, Y. Shono, and M. Hirabayashi, *Jpn. J. Appl. Phys.* **26,** L1727 (1987).

10. P. Zolliker, D. E. Cox, J. M. Tranquada, and G. Shirane, *Phys. Rev. B: Condens. Matter* **38,** 6575 (1988).

11. J. M. Tarascon, P. Barboux, P. F. Miceli, L. H. Greene, and G. W. Hull, *Phys. Rev. B: Condens. Matter* **37,** 7458 (1988).

12. F. Bridges, J. B. Boyce, T. Claeson, T. H. Geballe, and J. M. Tarascon, *Phys. Rev. B: Condens. Matter* **39,** 11603 (1989).

13. J. M. Tranquada, D. E. Cox, W. Kunnmann, H. Moudden, G. Shirane, M. Suenaga, P. Zolliker, D. Vaknin, S. K. Sinha, M. S. Alvarez, A. J. Jacobson, and D. C. Johnston, *Phys. Rev. Lett.* **60,** 156 (1988).

14. H. Yasuoka, T. Shimizu, Y. Ueda, and K. Kosuge, *J. Phys. Soc. Jpn.* **57,** 2659 (1988).

15. V. Sedykh, S. Nasu, and F. E. Fujita, *Solid State Commun.* **67,** 1063 (1988).

16. S. Nasu, M. Yoshida, Y. Oda, T. Kohara, T. Shinjo, K. Asayama, F. E. Fujita, S. Katsuyama, Y. Ueda, and K. Kosuge, *J. Magn. Magn. Mater.* **90** and **91,** 664 (1990).

17. M. Yoshida, Master thesis at Osaka University, 1990.

18. S. Nasu, H. Kitagawa, M. Yoshida, Y. Oda, K. Ueda, T. Kohara, T. Shinjo, K. Asayama, and F. E. Fujita, *Hyperfine Interact.* **55,** 1355 (1990).

19. S. Katsuyama, T. Kamiyama, H. Asano, F. Izumi, Y. Ueda, and K. Kosuge, unpublished work.

20. A. Nath, S. Nagy, M. W. Barsoum, S. D. Tyagi, and Y. Wei, *Solid State Commun.* **68,** 181 (1988).

21. A. Nath and Z. Homonnay, *Physica C* **161,** 205 (1989).

22. H. Mazaki, S. Katsuyama, H. Yasuoka, and K. Kosuge, *Jpn. J. Appl. Phys.,* **30,** 1386 (1991).

23. Z. Q. Qiu, Y. W. Du, H. Tang, and J. C. Walker, *J. Appl. Phys.* **67,** 5458 (1990).

24. M. G. Smith, R. D. Taylor, and H. Oesterreicher, *Phys. Rev. B: Condens. Matter* **42,** 4202 (1990).